

## Viral dynamics in transplant patients: implications for disease

Georg A Funk, Rainer Gosert, Hans H Hirsch

*Lancet Infect Dis* 2007; 7:  
460–72

Transplantation Virology,  
Institute for Medical  
Microbiology, University of  
Basel, Basel, Switzerland  
(G A Funk PhD, R Gosert PhD,  
Prof H H Hirsch MD); and  
Division of Infectious Diseases  
and Hospital Epidemiology,  
University Hospital Basel, Basel  
(H H Hirsch)

Correspondence to:  
Prof Hans H Hirsch,  
Transplantation Virology,  
Institute for Medical  
Microbiology, University of Basel,  
Petersplatz 10, CH-4003 Basel,  
Switzerland.  
Tel +41 61 267 3262;  
fax +41 61 267 3283;  
hans.hirsch@unibas.ch

Viral infections cause substantial morbidity and mortality in transplant patients. Quantifying viral loads is widely appreciated as a direct means to diagnose and monitor the course of viral infections. Recent studies indicate that the kinetics of viral load changes rather than single viral load measurements better correlate with organ involvement. In this Review, we will summarise the current knowledge regarding the kinetics of viruses relevant to transplantation including cytomegalovirus, Epstein-Barr virus, the herpes viruses 6 and 7, hepatitis C virus, GB virus C, adenovirus, and the emerging human polyomavirus type BK. We discuss the implications of viral kinetics for organ pathology as well as for the evaluation of antiviral interventions in transplant patients.

### Introduction

Viruses can cause organ pathology and disease through direct cytopathic effects of viral replication in host cells as well as through inflammatory processes, killing of infected cells by specific immune effectors, or induction of oncogenic transformation.<sup>1,2</sup> The introduction of molecular genetic tools, particularly PCR, has greatly simplified the sensitive and specific identification of viral agents and PCR is now widely available in the clinical routine. In the quantitative format, PCR allows for the direct measurement of viral loads in patient samples. In fact, monitoring viral loads over time reveals changes with onset and treatment of viral disease. In individuals with naive or impaired immune effectors, or both, viral loads are generally found to be higher and persist for longer periods. Mathematical models fitted to serial viral load measurements allowed parameters such as viral doubling times and half-lives *in vivo* following antiviral interventions to be estimated.<sup>3</sup> These viral dynamic parameters proved useful for predicting the risk of progression to organ failure and for estimating the efficacy of antiviral interventions.

The era of viral dynamics *in vivo* was inaugurated in 1995 by investigating HIV-1.<sup>4–6</sup> Since then, viral dynamics have been explored for several agents including chronic hepatitis B and hepatitis C viruses.<sup>7–9</sup> The common hallmark of these viral diseases is progressive organ dysfunction through persistent high-level virus replication in affected patients. In immunocompetent individuals, high-level replication is only transiently observed during acute primary infection, if at all. Chronic viral diseases do not only reflect specific viral characteristics, but also result from the inability of an individual's immune system to sufficiently control and clear the virus.

In transplant patients, impaired antiviral immune control results from deliberate pharmacological immunosuppression to counter immune injury (rejection), and from viral infection of HLA-mismatched allogeneic tissues. Both factors are particularly important in the setting of primary infection post-transplant—eg, in donor seropositive/recipient seronegative solid organ transplantation and in recipient seropositive patients after T-cell depletion or donor seronegative haematopoietic stem cell transplantation.<sup>10</sup> Finally, some viruses, such as cytomegalovirus (CMV), appear to actively contribute to a

quantitative and qualitative state of immunodeficiency,<sup>11</sup> which is paradigmatic for HIV through infecting and exhausting CD4+ T cells en route to the clinical state of AIDS.<sup>12</sup>

Quantification of HIV in blood samples indicated that high steady-state plasma viral loads following the acute phase of infection correlated with faster progression to AIDS.<sup>13</sup> Treatment with potent inhibitors of HIV replication revealed a multiphasic decline in plasma HIV-RNA, associated with different host cell compartments and biological states of infection (figure 1). Analyses of the declines indicated half-lives of 1–2 days (first phase decline), approximately 14 days (second phase decline), and 90–150 days or more (third phase decline).<sup>6,14–17</sup> Time to eradication was determined by the half-life of the slowest decaying infected cell population. The projected eradication time (to less than one virus) predicted lifetime persistence of HIV despite fully suppressive therapy.<sup>18–20</sup> Viral rebounds after cessation of therapy reflect recruitment of productively infected cells as the source compartment. The short viral half-life implied a high daily turnover (figure 2). The bulk of plasma HIV (more than 99%) is derived from productively infected cells, most of which are activated CD4+ T cells. With a productively infected cell half-life of approximately 1 day,<sup>21</sup> about 50% of those cells need to be produced and cleared

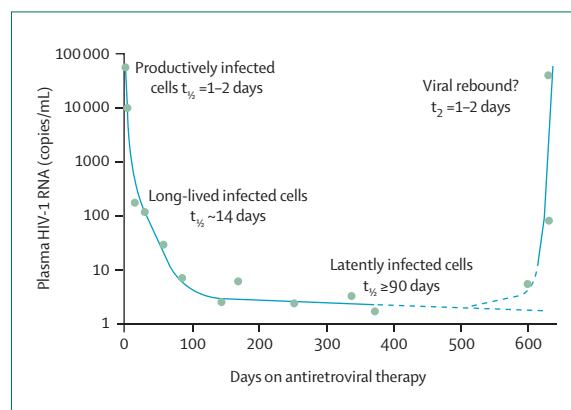


**Figure 1: HIV kinetics**

Half-lives can be estimated from the slope of the viral load decline after initiation of antiretroviral therapy. The dashed blue line indicates projection of the viral load decay below the limit of detection of the assay. Also depicted is a viral rebound after cessation of antiretroviral therapy.  $t_{1/2}$ =half-life.  $t_2$ =doubling time.

every day to maintain an apparently stable viral load. A small proportion of plasma virus (less than 1%) appears to come from long-lived infected cells. By contrast, latently infected cells do not contribute to viral loads unless reactivation reverts them into a virus-producing state.

### Viral dynamics in transplant patients

In transplant patients, decline of viral loads can be achieved not only by antiviral drugs, but also by modulating (reducing) immunosuppression. Temporary reduction in viral load may occur during surgical procedures—eg, during the short time-span between extraction of an infected graft and reperfusion of a new (uninfected) one. Similar to HIV studies, antiviral drug-induced perturbation experiments have been applied to quantify the “speed” of the viral turnover of three major pathogens in vivo—human CMV, hepatitis C virus (HCV), and Epstein-Barr virus (EBV)—and to link viral dynamics to disease progression. For human herpesviruses (HHV) 6, HHV7, GB virus C (GBV-C; also called hepatitis G virus), and adenovirus, viral load data have been published but the speed of the viral turnover was not established. Here, we have extracted the available data to estimate doubling times and half-lives (table 1).

### Human cytomegalovirus

CMV is one of the most significant viral pathogens after transplantation. Without antiviral treatment, the incidence of CMV replication ranges from 40% to 80% and more than half of transplant patients become symptomatic.<sup>23,43</sup> Consensus definitions were established to distinguish between active CMV infection (evidence of replication according to antigen or PCR testing), symptomatic infection defined as CMV syndrome (CMV

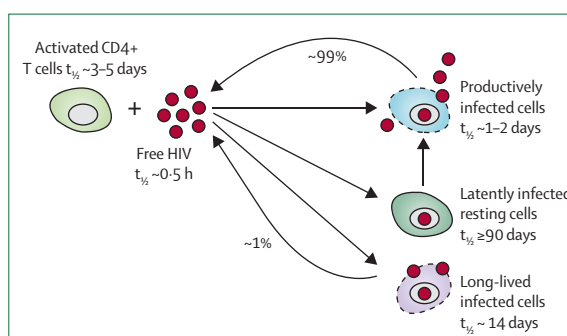


**Figure 2: HIV compartments**

Associated with the different viral decay half-lives are different host cell compartments and biological states of infection. The figure indicates the respective contributions to the plasma viral turnover.  $t_{1/2}$ =half-life.

replication plus fever, weakness, leucopenia, thrombocytopenia), and CMV disease (CMV replication and histological evidence of organ-invasive disease in liver, gastrointestinal tract, lung, etc).<sup>44</sup> These direct effects of CMV replication are distinct from the so-called indirect, part immunologically mediated effects, which include acute rejection episodes, bronchiolitis obliterans, graft vasculopathies, and fungal infections.<sup>11</sup> Major reservoirs of latent CMV infection in vivo are thought to be cells of the myeloid lineage. During active replication, the virus widens its host cell range and may replicate in many cell types including endothelial cells, but also organ-specific cells, which may give rise to specific manifestations in the lungs, liver, intestinal tract, and CNS. Reactivation might involve declining immune surveillance as well as activating stimuli—eg, inflammatory cytokines (tumour necrosis factor  $\alpha$ ) or ischaemia/reperfusion injury.<sup>45,46</sup>

	Intracellular delay	Transplant patients			Non-transplant patients			Viral generation time	References used to calculate kinetic estimates
		Doubling time	Half-life	$R_0^*$	Doubling time	Half-life	$R_0^*$		
Cytomegalovirus	Approximately 18 h (reference 22)	1-3 days	1-20 days	0.83-1.5	2 days	17 h to 3 days	0.5-1.3	$\geq 3$ days	23-26
Epstein-Barr virus	Not well defined	7 h to 3 days	16 h to 3 days	$>1-1.4$	..	1.7-2.6 h	..	..	27-30
Human herpesviruses 6	5-6 h	$\leq 10$ h	21 h	1.5	..	..	..	$\leq 16$ h	31
Human herpesviruses 7	5-6 h	$\leq 22$ h	1.8 days	1.2	..	..	..	$\leq 30$ h	31
Hepatitis C virus	$\geq 6$ h (reference 32)	7-35 h	0.2-10 h	$>2.2$	..	1.5-4.6 h	$>15$	$\geq 8$ h	9, 32-35
GB virus C	..	..	2.5-18 days	..	..	..	..	..	36
Polyomavirus type BK	2 days (reference 37)	18 h to 37 days	1-6 h	0.86-2.6	..	..	..	2-3 days	36
Adenovirus	$\geq 16$ h (reference 38)	1-3 days	0.05 h	1.4	..	..	..	$\geq 16$ h	39, 40
HIV-1	Approximately 1 day (reference 41)	..	..	..	..	0.5 h	2-20	1-2 days	6, 16, 32, 42

..=unknown. Viral doubling time, half-life, and estimated basic reproductive ratio ( $R_0^*$ ) calculated from data of transplant and non-transplant patients. \* $R_0^*$  estimates may be biased to a less than maximum number because viral load slopes are likely to be confounded by the length of the sampling interval, which was often more than or equal to 1-2 weeks.

**Table 1: Viral kinetics in transplant and non-transplant settings**

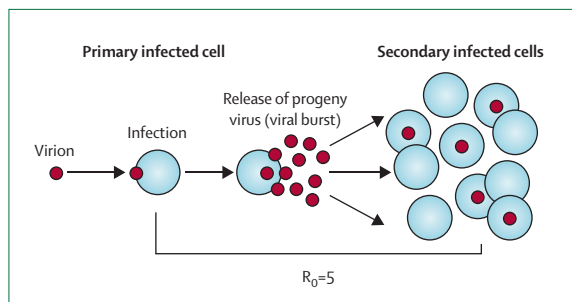


**Figure 3:** Schematic representation of the basic reproductive ratio in infection dynamics

$R_0$  quantifies the number of secondary infected cells per primary infected cell at the beginning of an infection when target cells are not yet a limiting factor. During chronic infection,  $R_0$  must be close to 1.  $R_0$  can be calculated from the viral growth rate,  $r$ , the length of the eclipse phase,  $e$ , and the average duration over which virus is released,  $d$ , by the formula  $R_0 = (1 + r \cdot d) \text{Exp}(r \cdot e)$ . For lytically replicating viruses, the formula simplifies to  $R_0 = \text{Exp}(r \cdot e)$ .

The association between CMV loads and clinical manifestations has been investigated. Both faster viral growth rates (ie, a shorter viral doubling time) and slower viral clearance rates (ie, a longer viral half-life) were associated with a higher likelihood of CMV disease. In a study of 127 CMV DNA-positive transplant patients (49 bone marrow, 47 liver, 31 kidney), Emery and colleagues<sup>24</sup> observed that the initial rate of increase of the viral load per mL whole blood correlated well with the risk of developing high viral load peaks and clinical disease. In this study, blood was sampled weekly during the first 3 months post-transplant and retrospectively analysed by quantitative PCR. Fewer than 10% of patients received ganciclovir for pre-emptive therapy. Patients who developed CMV disease (49 patients) had an initial viral doubling time of 2.1 days (range 10 h to 7 days), whereas patients who remained free of CMV disease had a lower doubling time of 3.6 days (range 1.4–23 days). CMV half-life estimates of approximately 17 h are available from five frequently sampled AIDS-patients (median five samples over 21 days) receiving ganciclovir therapy to treat CMV-associated retinitis.<sup>25</sup>

A study by Mattes and colleagues<sup>26</sup> comparing pre-emptive ganciclovir therapy with valganciclovir lent further support to the above estimates. CMV-DNAemia (defined by two consecutive CMV PCR results with at least 200 genomes per mL) was evaluated in 45 transplant patients at least twice weekly for 28 days. 23 patients (11 renal, 12 liver) received intravenous ganciclovir (5 mg/kg twice a day), whereas 22 patients (seven renal, 15 liver) received valganciclovir (900 mg twice a day). In the ganciclovir group, a viral doubling time of 2.0 days before treatment and a half-life of 1.7 days after initiation of therapy were observed. In the valganciclovir group, doubling time was reported as 1.8 days and half-life as 2.2 days. Although viral kinetics in the ganciclovir group were more favourable, differences were not significant.

Additional information on CMV dynamics in transplant patients can be derived from reports of Ghisetti and

colleagues<sup>23</sup> and Razonable and colleagues.<sup>47</sup> Liver and heart transplant patients received either oral ganciclovir therapy (1 g three times daily, adjusted for renal function) for 8 weeks,<sup>47</sup> or intravenous ganciclovir (10 mg/kg per day) for 21 days.<sup>23</sup> Razonable and colleagues<sup>47</sup> reported that eight of 25 patients developed CMV disease, but the authors did not provide detectable viral loads 1 week before onset of CMV disease. Within 7 days, CMV loads increased from less than 400 copies per  $10^6$  peripheral blood leucocytes to a median value of 16 300 copies per  $10^6$  peripheral blood leucocytes. We used the reported data to estimate a minimum viral load slope of 0.53 per day, which corresponds with a doubling time of 1.3 days or less (consistent with the data reported by Emery et al<sup>24</sup>). Here, it is worth noting that hampered viral replication under therapy was associated with diminished incidence of CMV disease when compared with a placebo control group. When calculating initial CMV doubling time from data provided by Ghisetti and colleagues,<sup>23</sup> we found a doubling time of 1.5 days in symptomatic patients compared with 21 days in asymptomatic patients. From three patients with biweekly sampling,<sup>23</sup> we estimated the following kinetic data: patient 1 (CMV disease), doubling time 2–3.5 days, half-life 4 days; patient 2 (CMV disease), doubling time 1.5–5 days, half-life 2.8–3.8 days. By contrast, patient 3 remained asymptomatic and was not treated with antiviral drugs. In this patient the dynamics seemed to be slow, since doubling time was 6–10 days whereas half-life was 7–12 days.

The relation between CMV clearance and disease recurrence was analysed in a study of 52 transplant patients (35 liver transplants, seven kidney, seven lung, and three others) with viral loads measured at least once per week.<sup>48</sup> CMV half-lives were quantified either after pre-emptive therapy with oral ganciclovir (2 g per day) or with intravenous ganciclovir (5 mg/kg per day), whereas patients with CMV disease were treated with intravenous ganciclovir (10 mg/kg per day). The mean viral half-life was 4.5 days (median 2.5 days, range 1–20 days). The study indicated that the probability of developing CMV disease recurrence was less than 7% in patients with rapid viral declines (half-life 3 days or less), but more than 55% for patients showing only slow CMV declines (half-life 7 days or more).

In infection epidemiology, the basic reproductive ratio ( $R_0$ ) describes the expansion of a transmittable agent or disease in a susceptible population and serves as a measure to assess intervention strategies including vaccinations.<sup>49</sup> The term may also be useful to quantitatively describe the biology of infectious agents within individuals. Here,  $R_0$  corresponds with the number of secondary infected cells per primary infected cell at the beginning of an infection (figure 3). Expanding viral populations (ie, increasing viral loads) are characterised by  $R_0 > 1$ , whereas contracting virus populations (ie, declining viral loads) are characterised

by  $R_0 < 1$ . In patients with persisting viraemia but a stable viral load,  $R_0 = 1$ . A thorough discussion of  $R_0$  in various infectious disease dynamics models has been provided by Lloyd.<sup>50</sup>

To illustrate the use of  $R_0$  for CMV, we assumed an intracellular delay of 18 h according to in-vivo data from an animal model.<sup>22</sup> On the basis of our estimates of the CMV doubling time from the data of Razonable and colleagues,<sup>47</sup> we calculated that  $R_0$  is 1.5 or more during the 7 days between undetectable viral loads and onset of disease. For the three patients detailed above from Ghisetti and colleagues,<sup>23</sup> we estimated that ganciclovir therapy in patient 1 is 24% effective ( $R_0$  decreased from 1.16 to 0.88). In patient 2, the efficacy of the first treatment episode is 22% ( $R_0$  1.11 to 0.87), whereas that of the second treatment episode is 43% ( $R_0$  1.45 to 0.83). For the patients detailed in the study by Mattes and colleagues,<sup>26</sup> we estimated that ganciclovir was 43% effective ( $R_0$  1.29 to 0.74), whereas valganciclovir was 41% effective ( $R_0$  1.33 to 0.79). In patient 3 from Ghisetti and colleagues' study,<sup>23</sup> who remained asymptomatic and did not receive treatment, increasing immune control or decreasing activating stimuli resulted in an efficacy of less than 15% ( $R_0$  1.09 to 0.93).

Taken together, CMV replication dynamics suggest that short doubling times in the order of 2 days seem to predict a higher risk for CMV disease than doubling times of 4 days or more. Conversely, successful intervention for CMV replication and disease was more likely in patients with more rapidly declining CMV loads (half-life less than 4 days). Although these kinetic parameters were observed in patients treated with CMV-specific antiviral drugs, they might include as yet unquantifiable effects of reduced immunosuppression and immune responses. Using  $R_0$ , net efficacies of all interventions ranged from 22% to 43%. The use of  $R_0$  may also help to understand cases where antiviral drugs have caused a replacement of the wildtype strain as the prominent species by slower growing drug-resistant strains with reduced fitness and less pathogenic potential.<sup>51</sup>

### Epstein-Barr virus

EBV-specific T-cell function has a key role in the control of EBV replication and latency. Intense immunosuppression, the use of T-cell depleting agents for induction or treatment, HLA-mismatches, and primary EBV infection are key risk factors for EBV disease, and particularly, post-transplant lymphoproliferative disorders (PTLD). The pathogenesis of PTLT is complex and involves progression from a polyclonal B-cell proliferation to oligoclonal and monoclonal malignant stages.<sup>52,53</sup> EBV-encoded gene products function as oncogenes driving the proliferation of B cells.<sup>54</sup> Uncontrolled EBV replication might add to the risk for subsequent malignant transformation through extensive infection and recruitment of B cells. Surveillance of EBV

loads in plasma, whole blood, and peripheral blood mononuclear cells has been widely used to identify transplant patients at risk for EBV-associated PTLT and to guide therapeutic interventions, which include reducing immunosuppression, chemotherapy, and/or immunotherapy.<sup>55</sup> Only a lesser but variable fraction of the blood viral load is derived from lytic EBV replication, whereas the pathologically more relevant load is derived from transformed host B cells.

No kinetic data are available for EBV in the transplant setting. To approximate EBV kinetics, we selected four papers with sufficient data. In a first step, we extracted the minimum EBV-DNA doubling time and half-life from the data without taking into account episomal or lytic origins (table 2). In a second step, we considered different scenarios of episomal and lytic contributions to EBV load (figure 4).

In the first paper, Smets and colleagues<sup>27</sup> screened 45 paediatric liver transplant patients. In patients with PTLT, immunosuppression was stopped but reintroduced later in some cases. In patients with CMV or EBV disease, aciclovir (30 mg/kg per day) given during the first year was switched to intravenous ganciclovir (10 mg/kg per day) for 14–21 days. From the data reported,<sup>27</sup> we obtained minimum estimates of doubling times and half-lives after primary EBV infection of approximately 2 days (table 2).

	Doubling time	Sampling interval	Half-life	Sampling interval	Intervention
<b>Smets et al (2002),<sup>27</sup> liver transplanted children</b>					
Patient 1	Approximately 2 days	Week 2–4	7 days	Week 8–10	Aciclovir then ganciclovir
Patient 2	≤4 days	Week 2–8	3 days	Week 12–15	Aciclovir then ganciclovir
Patient 3	≤3 days	Week 2–6	1.6 days	Week 6–8	Aciclovir then ganciclovir
Patient 4	≤5 days	Week 2–8	..	..	Aciclovir then ganciclovir
<b>Gärtner et al (2002),<sup>28</sup> stem cell transplantation</b>					
Patient 1	2.7 days	Day 36–63	..	..	Foscarnet, ganciclovir
Patient 3	1.2 days	Day 36–55	..	..	Foscarnet, ganciclovir
Patient 4	2.7 days	Day 70–100	..	..	Foscarnet, ganciclovir, aciclovir
Patient 8	Approximately 21 h	Day 42–54	..	..	Aciclovir
<b>Gustafsson et al (2000),<sup>56</sup> bone marrow transplants</b>					
Patient 1	1.8 days	Day 21–42	..	..	CTL infusion
Patient 2	2.5 days	Day 21–50	..	..	CTL infusion
Patient 3	..	..	≤1 day	Day 147–154	CTL infusion
Patient 4	≤3 days	Day 21–45	..	..	CTL infusion
Mean (SD)	≤2.6 (1.2) days		≤3.2 (2.7) days	..	
..=unknown. EBV-DNA doubling time and half-life was calculated from the indicated sources. The mean (SD) is across all patients. CTL infusion=infusion of ex-vivo expanded EBV-specific cytotoxic T lymphocytes.					
<b>Table 2: Kinetic estimates of EBV calculated from published work</b>					

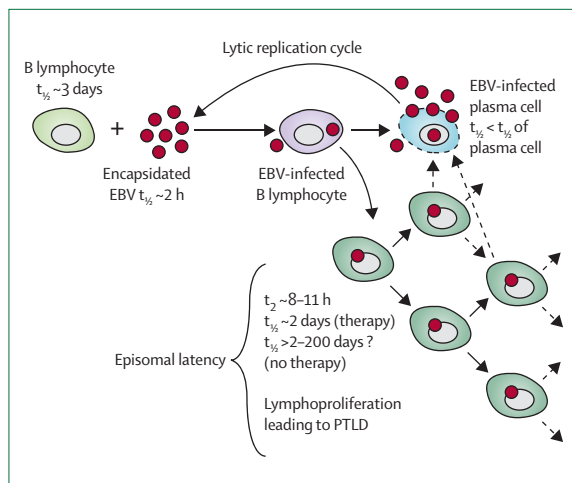


**Figure 4: B-cell PTLD compartments**

Upon primary infection of uninfected B cells with EBV, infected host cells enter the lymphoproliferative cycle. It is characterised by episomal latency of EBV. Immunocompromised individuals may eventually progress to PTLD. EBV appears to switch to lytic replication if infected host cells differentiate into (short-lived) plasma cells. EBV=Epstein-Barr virus. PTLD=post-transplant lymphoproliferative disorders.  $t_{1/2}$ =half-life.  $t_2$ =doubling time.

Treatment with antiviral drugs such as aciclovir (1600 mg per day orally or 750 mg per day intravenously), foscarnet (induction 120 mg per day, maintenance 90 mg per day), and ganciclovir (10 mg/kg per day) was used by Gärtner and colleagues<sup>28</sup> who evaluated EBV loads of 59 stem cell transplant patients as a parameter for prediction and monitoring of PTLD. From this study, we estimated a minimum doubling time of about 21 h (table 2). In one adult patient, EBV doubling time was approximately 11 h (day 29–36), and half-life around 16 h (day 57–65, aciclovir discontinued, foscarnet and ganciclovir started). In one paediatric patient with primary EBV infection, doubling time was approximately 23 h (day 28–36) and half-life around 1 day (day 50–59, aciclovir discontinued). Thus, the estimates of the shortest EBV dynamics yielded doubling time of approximately 11 h and half-life approximately 16 h. In these preliminary estimates, no effect of antiviral treatment could be discerned, but the sampling frequency may not have been adequate for further conclusions. Despite antiviral therapy, EBV dynamics were rapid with the shortest viral doubling time similar to B-cell proliferation times of 8–11 h.<sup>57</sup>

Changes in EBV loads after administration of anti-CD20 antibodies (rituximab) were reported by Orentas and colleagues.<sup>29</sup> One paediatric bone marrow transplant patient had—within 1 day—a rapid initial response to rituximab followed by a rapid rebound of EBV load ( $1.65 \times 10^6$  to  $2.06 \times 10^5$  to  $7.40 \times 10^5$  copies per  $\mu\text{g}$  DNA).<sup>29</sup> Assuming equally long time intervals for the decay and rebound phase at day 83 (otherwise one estimate would get shorter at the expense of the other one), the half-life was about 4 h, and the doubling time during the viral rebound the same day was around 7 h. The half-life after a second anti-CD20 injection at day 88 was 8 h or less

( $1.179 \times 10^6$  to  $1.5 \times 10^5$  copies per  $\mu\text{g}$  DNA). The short half-life of approximately 4 h is similar to median plasma viral load decline half-life of approximately 2 h observed after surgical resection of nasopharyngeal carcinomas.<sup>30</sup>

Adoptive immunotherapy has been applied by Gustafsson and colleagues<sup>56</sup> who studied how infusion of EBV-specific cytotoxic T cells reduced EBV-DNA loads in nine bone marrow transplant patients, thereby diminishing the risk of PTLD. Kinetic parameters estimated from this study were doubling time approximately 1.8 days and half-life 1 day or less (table 2). The two studies<sup>29,56</sup> show that immune therapy is powerful in reducing cell-associated viral loads. However, fast rebounds reported in these studies raise questions about the duration of response.

We note that the average doubling time of EBV across different transplant settings and interventions was remarkably robust (mean doubling time 2.6 [SD 1.2] days or less, table 2). To estimate B-cell PTLD dynamics in vivo, we provide preliminary estimates of the daily loss of EBV-infected cells if EBV replication were entirely episomal, if EBV replication were only lytic, or if both modes were mixed (figure 5). 1  $\mu\text{g}$  DNA corresponds with around 150 000 cells (using the standard conversion factor of 6.6 pg DNA per diploid cell).<sup>29</sup> Wagner and colleagues<sup>58</sup> report a median EBV load of 50 copies per  $\mu\text{g}$  DNA in immunocompetent (healthy) EBV-seropositive carriers. This corresponds with a frequency of one EBV copy per  $3 \times 10^3$  cells. Assuming that an adult individual has approximately  $10^{11}$  B cells,<sup>59</sup> this amounts to  $3.3 \times 10^7$  EBV copies per individual. Applying an EBV half-life of 2 days as extracted from the data of Smets and colleagues,<sup>27</sup> we estimate that about  $9.7 \times 10^6$  EBV copies, or 30%, were cleared every day. Assuming a purely episomal mode of EBV-DNA replication in dividing B cells, and only one episome per cell, the turnover is approximately  $9.7 \times 10^6$  cells per day under conditions of stable EBV loads (figure 5). If a cell contains 20 episomes,<sup>60</sup> the daily turnover is 20 times lower. If the daily declining EBV load corresponded with loss of cells alone and was to be balanced by three cell divisions per day,<sup>57</sup> approximately  $6.1 \times 10^4$  to  $1.2 \times 10^6$  cells needed to proliferate. Under steady-state conditions, it is clear that the daily loss of B cells decreases if the half-life of an infected cell increases. Because the fraction of lytically replicating cells also affects the daily loss of B cells, we plotted in figure 5 how a switch from entirely episomal replication over mixed modes to purely lytic replication influences cell loss, assuming that 5000 progeny viruses were released per lysed host cell and a virion half-life of 2 h. The calculated turnover rate for a cell half-life of 33 days and about 12% lytic replication is around four B cells per second (figure 5). For the given viral burst size, a switch from episomal to lytic replication does not much alter estimated B-cell turnover rates as long as the proportion of lytically replicating cells remains at 75% or less.

During the peak of primary EBV infection, average EBV copy numbers are around 2000-fold higher

compared with EBV levels of healthy seropositive carriers.<sup>28</sup> Thus, extrapolations indicate that at peak of infection, 10% or more of all B cells can be EBV positive and that peak body cell loss values can be  $10^3$  or more times higher than those indicated in figure 5. Considering that the blood contains about 1.4% of B cells,<sup>59</sup> our estimates are in line with values of tonsillar (approximately  $135 \times 10^7$ ) and peripheral blood (approximately  $175 \times 10^7$ ) EBV-infected cells measured by Laichalk and colleagues.<sup>61</sup>

PTLD sometimes progresses very rapidly leading to death of an individual within 1 month.<sup>28</sup> Our dynamic view of the B-cell PTLT implies that to grow within 30 days after initiation of transplantation-immunosuppression from around  $10^7$  EBV-positive cells, as reported from healthy EBV-seropositive individuals,<sup>58</sup> to around  $10^{11}$  EBV-positive cells—ie, doubling the abundance of B cells in vivo—the net growth rate (Malthusian parameter) must be approximately 0.31 per day. This corresponds with a net doubling time of approximately 2.2 days (panel and figure 6).

In summary, we find rapid EBV dynamics in the order of hours to around 2 days when comparing kinetic data of cell-free virus in non-transplant patients where the source of viral replication was removed with estimates of cell-associated virus obtained from antibody or cytotoxic-T-lymphocyte-treated transplant patients. The shortest viral doubling times of cell-associated EBV-DNA of 7–11 h match the doubling times of proliferating B cells.<sup>57</sup> Our estimation of the daily EBV-associated B-cell turnover hinged on the assumption of a dynamic steady-state. Under conditions described in figure 5, the turnover in a healthy EBV-positive individual is one to four B cells per second. The variable kinetics of PTLT progression observed in patients can be explained by differences in the net surplus between proliferating cells and destructed cells. This could also explain the rapid doubling of the tumour mass and difficulties with debulking treatment necessitating surgery and chemotherapy. The accumulation of EBV-infected cells could be circumvented by avoiding T-cell depleting protocols or by infusing ex-vivo expanded EBV-specific T cells to check uncontrolled B-cell proliferation.<sup>62,63</sup>

#### Other transplant relevant herpesviruses

The majority of adults are seropositive for HHV6 and HHV7. Primary infection usually occurs during early childhood and infected individuals remain persistently infected throughout life. The main target cells of both viruses seem to be CD4+ mononuclear cells and cells of salivary glands. Reactivation in immunocompromised hosts might be responsible for opportunistic diseases. In stem cell transplant recipients, HHV6 has been associated with fever, encephalitis, interstitial pneumonitis, delayed engraftment, and high graft-versus-host disease. The pathological potential of HHV7 in this setting is less well defined. Boutolleau and colleagues<sup>31</sup> assessed the level of

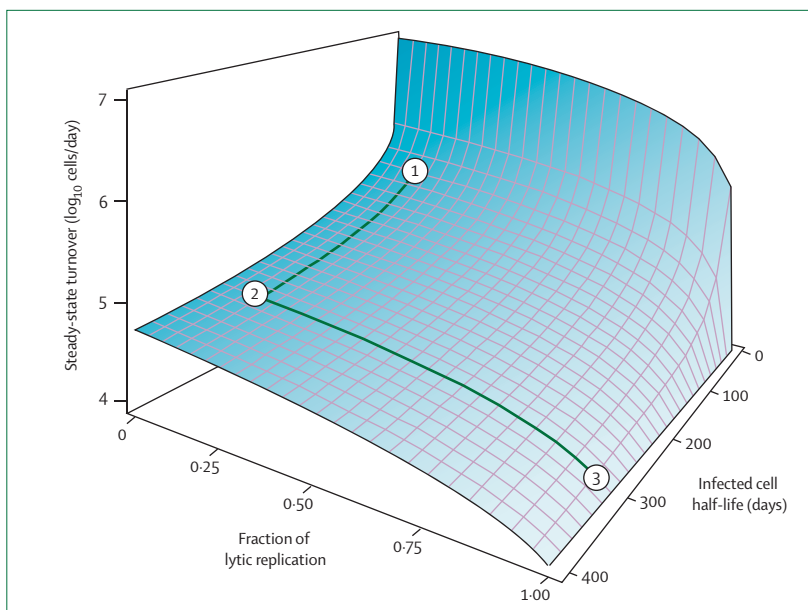


**Figure 5: Daily loss of B cells in healthy EBV-seropositive individuals**

Steady-state EBV load: equivalent to 50 copies per  $\mu\text{g}$  peripheral blood mononuclear cell DNA. Circles indicate selected points: (1) 12% lytic replication, half-life 33 days (corresponding cell loss approximately  $5.5 \log_{10}$  cells per day, equivalent to four cells per second); (2) 12% lytic replication, half-life 300 days (corresponding cell loss approximately  $4.8 \log_{10}$  cells per day, equivalent to 0.8 cells per second); (3) 96% lytic replication, half-life 300 days (corresponding cell loss approximately  $4.2 \log_{10}$  cells per day, equivalent to approximately 0.5 cells per second). Note that changes in the proportion of lytic replication between 0–75% do not substantially alter B-cell turnover rates. We assume that 5000 progeny viruses are released per lytically infected cell; virion half-life 2 h. Total B cells per individual:  $10^{11}$  cells. Colour code shows darker blue=high values; lighter blue=low values. The plot was generated with a two dimensional function  $f(x,y) = \log_{10}[x(t_0,p) + y(t_0,p)]$ , with  $x(t_0,p)$  considering cell loss caused by episomal replication and  $y(t_0,p)$  considering cell loss caused by lytic replication.  $t_0$ =half-life.

viral replication in 78 stem cell transplant patients post-transplant. The median follow-up was 107 days, and post-transplant peripheral blood mononuclear cell samples were collected every 7–14 days. All patients received aciclovir prophylaxis against CMV infection. In a subset of 66 patients, sufficient data for HHV6 and HHV7 kinetic estimates were described.<sup>31</sup> On the basis of median viral load data, we obtained an HHV6 doubling time of 1.6 days (day 0–7) and 3.2 days (day 7–14) and a half-life of 1.9 days (day 14–21). Analysis of the HHV6 growth kinetics of patient 1, who had a tremendous viral expansion followed by a stable viraemia,<sup>31</sup> revealed a rapid increase with a doubling time of 10 h or less over the first 6 days and a doubling time of about 4.5 days between days 6 to 21. Growth kinetics were similar in patients 2 and 3 (doubling time approximately 1.5 days), whereas the viral half-life between days 26 to 33 estimated from patient 2 was 21 h or less.<sup>31</sup> In all three cases, transient thrombocytopenia was observed about 2 weeks after the onset of HHV6 expansion. Additionally, delayed engraftment, cutaneous rash, and partial myelosuppression were associated with elevated viral load measurements.

From the median HHV7 viral load measurements reported by Boutolleau and colleagues,<sup>31</sup> we obtained a doubling time of 1.6 days (day 0–7) and half-life 1.8 days (day 7–14). The viral doubling time of HHV7 between day 0

**Panel: Mathematical model of EBV-associated PTLD**

A mathematical model was constructed to describe the dynamics of EBV-infected B cells (equation 1) and free virus (equation 2) en route to PTLD.

$$d/dtB_v = p^*B_v + i^*V^*B - d^*B_v - k^*T^*B_v \quad (\text{equation 1})$$

$$d/dtV = n^*d^*B_v - c^*V \quad (\text{equation 2})$$

The term  $p^*B_v$  denotes proliferation of EBV-infected B cells,  $i^*V^*B$  denotes infection of uninfected B cells by virus,  $d^*B_v$  lysis of infected B cells,  $k^*T^*B_v$  killing of infected B cells by immune effectors such as cytotoxic T lymphocytes,  $n^*d^*B_v$  release of viral progeny from lysed host cells, and  $c^*V$  clearance of free virus.

Assuming that the dynamics of free virus is much faster than that of infected cells, we can set  $d/dtV=0$ , solve for  $V$ , and replace  $V$  in equation 1. We then obtain a single equation describing the dynamics of EBV-infected B cells, which is

$$d/dtB_v = p^*B_v + i^*(n^*d^*B_v / c) * B - d^*B_v - k^*T^*B_v \quad (\text{equation 3}).$$

Factoring out  $B_v$  in equation 3 leads to

$$d/dtB_v = B_v * [p + (i^*n^*d^*B_v / c) - d - k^*T] \quad (\text{equation 4}).$$

From equation 4, we obtain the basic reproductive ratio as

$$R_0 = p / (d + k^*T) + i^*n^*d^*B_v / (c^*[d + k^*T]) \quad (\text{equation 5}).$$

The term  $p/(d+k^*T)$  denotes the contribution from episomal replication,  $i^*n^*d^*B_v/(c^*[d+k^*T])$  the respective contribution from lytic replication. If EBV replicates purely episomal (no lysis),  $R_0$  reduces to  $p/(k^*T)$ . To have  $B_v$  growing,  $R_0$  must be  $>1$  ( $B_v \neq 0$ ).

The formula for  $R_0$  provides a rationale to discuss the effect of various interventions on growth control of EBV-infected B cells. For a mixed mode of 10% lytic and 90% episomal replication, as shown in figure 6, the depletion of B cells by an anti-B220 antibody would reduce  $R_0$  from 1.16 to 1. Remission of a tumour requires additional simultaneous interventions such as chemotherapy with proliferation inhibitors or the infusion of ex-vivo expanded autologous T cells. For example, a 10% expansion of the EBV-specific T cells would further reduce  $R_0$  to about 0.91 (equivalent to a half-life of 5–6 days).

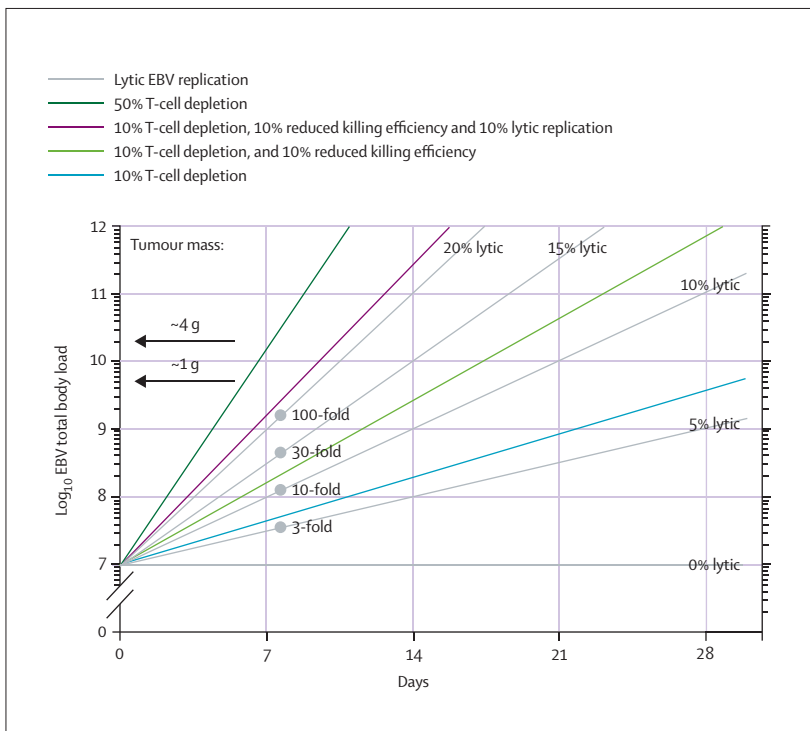


**Figure 6: Increase of EBV load en route to PTLD**  
 The horizontal grey line (labelled 0% lytic) indicates the steady-state EBV load of an immunocompetent healthy EBV-seropositive individual (equivalent to about 50 copies per  $\mu\text{g}$  DNA<sup>27</sup>). A switch from 100% episomal replication to a mixed mode of 5% lytic and 95% episomal replication increases the viral load by a factor of three within 1 week (see the line labelled 5% lytic). Higher fractions of lytic replication further increase the viral load. Coloured lines show the effect of various interventions on growth control of EBV-infected B cells. The diagram can be used as a graphical calculator to extrapolate the time until a critical tumour mass will be achieved in a patient.  $5 \times 10^9$  EBV-positive B cells correspond with a tumour mass of about 1 g,  $2 \times 10^{10}$  EBV-positive B-cells to a tumour mass of about 4 g. Parameters at steady-state:  $p=2.1$ ,  $i^*B=3.3$ ,  $n=5000$ ,  $d=0.00016$ ,  $c=8$ ,  $k=0.03$ ,  $T=70$ ,  $B_v(0)=1 \times 10^7$ .

to 7 in patient 3 was 22 h or less, the half-life between days 7 to 21 was approximately 2.1 days.<sup>31</sup> In general, viral loads were rather low, often below the limit of detection. No association between HHV7 infection and clinical or biological manifestations was observed.

The reported data suggest rapid dynamics of both HHV6 and HHV7 in stem cell transplant patients despite aciclovir prophylaxis. Preferentially, HHV6 seemed to reactivate in immunosuppressed patients, but this needs further study. CD4+ mononuclear cells, including CD4+ T cells, may be affected by HHV6 and HHV7 infection, but the precise relation of HHV6 and HHV7 kinetics on immune dysregulation requires further study. Individuals with prolonged high viral loads might require early treatment with antiviral drugs such as foscarnet, ganciclovir, or cidofovir.<sup>64,65</sup>

**Hepatitis C virus**

Liver failure resulting from chronic HCV infection is the main indication of liver transplantation today. The major challenges are complex treatments at substantial costs, but limited efficacy, particularly for genotype 1, which is associated with the poorest prognosis.<sup>66,67</sup> Patients treated with interferon  $\alpha$  frequently have depressive complaints. Of the 200 million people infected with HCV, only a minority lives in countries with transplantation centres. In addition to donor organ shortage, reinfection of the allograft is almost inevitable and graft failure because of recurrence of HCV is the most common cause of retransplantation.

Two types of kinetic estimates obtained from non-transplant patients support the hypothesis of a high viral turnover of HCV. In two HIV/HCV-infected patients

undergoing plasma apheresis, the half-life of HCV was 1.7 h and 3 h, as described in Ramratnam and colleagues.<sup>33</sup> During apheresis (duration 78–207 min), each patient had 25–30 viral load measurements. Similarly, rapid HCV kinetics were observed by Neumann and colleagues<sup>9</sup> in 23 HCV-positive patients treated with interferon alfa-2b (5, 10, or 15 million IU interferon alfa-2b for 2 weeks; sampling every 2–4 h for the first 2 days, then daily for 2 weeks).<sup>9</sup> The mean half-life was 2.7 h (range 1.5–4.6 h). The immediate efficacy of interferon alfa-2b was 80% or more, but dropped to 5–10% or less after 2–3 days. Different HCV genotypes have different interferon response elements leading to distinct decay kinetics under therapy.<sup>66</sup> Thus, the duration of therapy should be chosen according to the HCV genotype. The data indicate rapid dynamics of HCV in non-transplant patients.

In transplant patients, HCV is known to reinfect the newly transplanted liver allograft. Frequent sampling during and immediately after the anhepatic phase of liver transplantation provides unique insights into the replication dynamics of HCV. Fukumoto and colleagues<sup>34</sup> presented data of nine liver transplant patients with sampling 1 day before transplantation, then daily for up to 30 days post-transplant. During the first week post-transplant, all patients received antithymoglobulin and a combination of prednisolone, azathioprine, and cyclosporin A or tacrolimus for the next 3 weeks. The mean HCV half-life was about 4 h (range 2–5.2 h). In eight patients, viraemia began to increase around day 3 post-transplant and HCV-RNA levels exceeded the preoperative values by day 8.

Gracia-Retortillo and colleagues<sup>35</sup> also analysed data with sampling at the beginning and at the end of the anhepatic phase, followed by 4 h intervals for the first day after graft reperfusion, then daily for another 5 days, and weekly sampling for the next 3 weeks. All 20 patients received 0.5–1 g of methylprednisolone during transplantation. Thereafter, 13 patients received cyclosporin A or tacrolimus plus corticosteroids (regimen A), whereas the remaining seven patients received tacrolimus, mycophenolate mofetil, and monoclonal anti-interleukin-2 receptor antibodies (regimen B). During the anhepatic phase (45–207 min), viral loads decreased in 18 of 20 patients. The estimated mean half-life during the anhepatic phase was 2.2 h (range 0.22–10.3 h). However, in two of 20 patients (regimen A), viral loads remained stable during the anhepatic phase, suggesting that the removed graft was not the major source of plasma virus. After graft reperfusion, viral loads decreased for the first 8–24 h with a mean half-life of 3.4 h (range 0.71–12.8 h) in 19 of 20 patients (including the two patients with stable viraemia during the anhepatic phase). Subsequently, a rapid viral increase was observed in ten of 20 patients (eight on regimen A), with a mean doubling time of 13.8 h (range 7–35 h), and pretransplant viral loads were reached by day 4 post-transplant. Four of 20 patients

maintained a stable reduced viraemia (all on regimen A), and six patients showed a slower second-phase decline (no quantitative information available). It should be noted that five of six patients with a second-phase decline were on regimen B. 1 week after transplantation, viral load concentrations increased progressively in 15 of 20 patients (regimen A, nine; regimen B, six), and reached a plateau exceeding pretransplant values by the first month post-transplant. The total follow-up time was 24 weeks, but the study did not aim to relate virus kinetics with graft function. When assuming an intracellular delay of 8 h for HCV,<sup>32,35</sup> we estimate  $R_0$  to be in the order of 0.06 during viral contraction (anhepatic phase, half-life 2 h), whereas  $R_0$  is approximately 1.5 during the subsequent viral expansion driven by reinfection of the allograft (doubling time 14 h).

The stable viraemia during the anhepatic phase in two patients detailed in the study by Garcia-Retortillo and colleagues<sup>35</sup> suggests the existence of an extrahepatic replication compartment. Further evidence for extrahepatic HCV replication was obtained by Dahari and colleagues,<sup>32</sup> who analysed data of 30 liver transplant patients (including the 20 patients from the study by Garcia-Retortillo et al). By fitting mathematical models to data beyond the period of the anhepatic phase, evidence for extrahepatic HCV replication was found in more than 50% of the patients. The mean half-life of productively infected extrahepatic cells was estimated to be 2.6 days (range 0.7–5.3 days), and its contribution to the total plasma viral load was approximately 3% (range 0.1–14%).<sup>32</sup> Figure 7 shows the current view of HCV compartmentalisation.

HCV-associated pathology in the setting of transplantation-immunosuppression was studied in 51 renal transplant recipients.<sup>68</sup> Patients were not treated with interferon  $\alpha$  or ribavirin, but cyclosporin A was part of the immunosuppressive regimens. Serial biopsies of the native liver suggested that neither HCV-RNA levels nor the duration of infection were correlated with progression to liver fibrosis. This appears to be inconsistent with a dynamic appreciation of disease progression and organ pathology. Unfortunately, detailed HCV kinetic data in renal transplant recipients were not available, which would allow the effect of HCV dynamics or immunopathology to be distinguished. Possible explanations for the discrepancy are (1) a biopsy bias because of the focal nature of the disease, (2) cyclosporin A might inhibit HCV replication by binding to cyclophilin B, a functional regulator of the HCV RNA polymerase NS5B,<sup>69</sup> and (3) immunopathology contributes to liver fibrosis. A confounding effect of cyclosporin A on the data cannot be excluded, because a trend ( $p=0.08$ ) between duration of infection and progression to fibrosis was found.<sup>68</sup> The observation that HCV levels remained substantially elevated after renal transplantation suggests that the immunosuppressive effect of cyclosporin A overrides the inhibitory effect on HCV replication.<sup>68</sup>



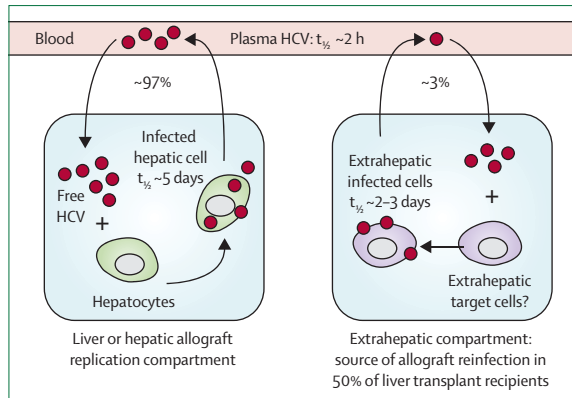


**Figure 7: HCV dynamics in vivo**  
 According to reference 32, the bulk of HCV in the plasma (around 97%) comes from replication in the hepatic compartment (left), and around 3% may come from an extrahepatic replication compartment (right). HCV=hepatitis C virus.  $t_{1/2}$ =half-life.

Taken together, the data indicate a high daily turnover rate of HCV in vivo of 99% or more. The data point to the liver as the principal site of HCV replication. The abundance of infected hepatocytes after liver transplantation was estimated to be 19%,<sup>70</sup> which compares with values of 30% or less estimated from chronic HCV-infected non-transplant patients.<sup>71</sup> Mathematical models suggest that in 50% or more of liver transplant recipients a second, slowly decaying extrahepatic replication compartment must exist.<sup>32,70</sup> Rapid reinfection of a new allograft with virus from the extrahepatic source is a major concern, which might be amenable to new potent drugs such as protease inhibitors that will be well tolerated before and after liver transplantation. Without antiviral treatment, the kinetics of viral decay and reinfection appear to be rapid, with a better viral control in patients in whom corticosteroids

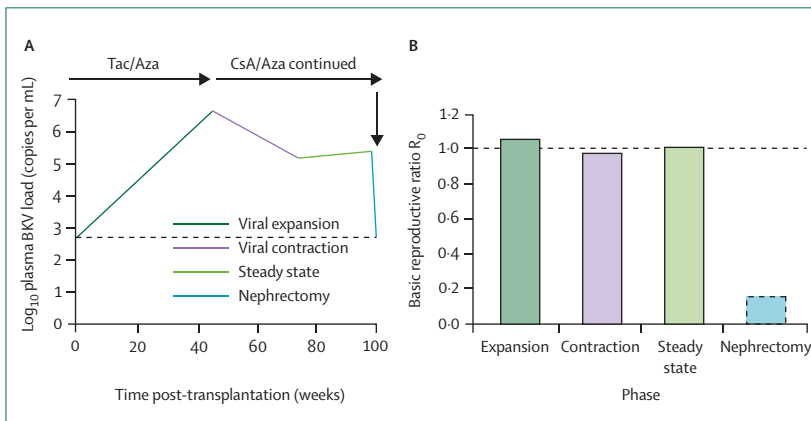


**Figure 8: BKV load changes in a kidney transplant recipient over 102 weeks post-transplant**  
 (A) Four phases are depicted. The immunosuppressive regimen is indicated at the top of the panel, transplant nephrectomy is indicated by a vertical black arrow, the detection limit of the assay is indicated by the horizontal dashed line. (B) Quantification of the efficacy of the interventions using the basic reproductive ratio  $R_0$  for the four phases. Upon nephrectomy,  $R_0$  drops to 0.2 or less. The dashed line at  $R_0=1$  indicates the threshold separating viral growth from viral decline.  $R_0$  is calculated according to the formula  $R_0 = \text{Exp}(s \cdot t_i)$ , with  $s$  denoting the slope of the viral load curve and  $t_i$  the intracellular delay. Tac=tacrolimus. CsA=cyclosporin A. Aza=azathioprine.

were not part of the immunosuppressive regimen. With treatment, a rapid decline of plasma HCV was associated with an amelioration of liver fibrosis scores.<sup>72</sup> However, this observation does not exclude immunopathology as an important cofactor in liver fibrosis and organ loss.<sup>73</sup>

**Polyomavirus type BK**

Polyomavirus infection is widespread in the general population with an age-dependent polyomavirus type BK (BKV) seroprevalence ranging from 60% to 90%.<sup>74</sup> Unlike herpesviruses, polyomavirus replication is largely dependent on host cell factors. It does not encode typical antiviral drug targets such as thymidine kinases or viral DNA polymerase. In replication-permissive cells, expression of the viral capsid proteins is followed by virion assembly in the nucleus, which eventually results in host cell lysis to release infectious progeny. By contrast with HIV, where lymphoid tissues in many anatomical sites are infected, graft nephrectomy studies in kidney transplant recipients indicate that the principal site of BKV replication is the renal allograft.<sup>75-77</sup> When manifest as a disease—a newly recognised cause of early allograft loss—it is called polyomavirus associated nephropathy (PVAN).<sup>73,78-81</sup>

The relation between the level of BKV replication, development of PVAN, and graft failure is not well understood.<sup>2,82</sup> First analyses indicate that BKV loads in plasma above  $10^4$  copies per mL are 93% sensitive and specific for histologically manifest disease.<sup>83</sup> However, false-negative biopsy results presumably caused by the focal nature of the infection have been obtained in around 30% of individuals.<sup>83</sup> In patients clearing BKV load in plasma, PVAN is no longer found histologically. Because no specific antiviral treatment is established, first-line treatment aims at improving the immune control by reducing immunosuppression.

Recently, we explored the dynamics of BKV in three nephrectomised and 12 non-nephrectomised patients receiving reduced immunosuppression.<sup>77</sup> Four different phases of BKV replication kinetics can be distinguished, as shown for one patient (figure 8). During the viral expansion phase between weeks 0 and 45, the BKV load increased from undetectable to a peak value of  $3.8 \times 10^6$  copies per mL. During that time the patient received tacrolimus and azathioprine as immunosuppressive therapy. From the slope of 0.025 per day of a fitted regression line, we estimated that the net viral doubling time was 28 days. Assuming an intracellular delay of 2 days from de novo infection of host cells to release of progeny virus,<sup>37</sup> we estimated that  $R_0$  was 1.05 (figure 8). When tacrolimus was replaced by cyclosporin A at week 45 (but azathioprine was continued), a phase of viral contraction lasting 29 weeks was observed. From the slope of  $-0.015$  per day, a net half-life of 45 days could be estimated, and  $R_0$  dropped to 0.97. Over the following 25 weeks, the BKV load remained stable at about  $10^5$  copies per mL indicating a quasi-steady-state

phase with an  $R_0$  of approximately 1. Because the slope of a fitted line would be close to zero during that time, no meaningful viral doubling time or half-life could be estimated. At week 99, the allograft was removed from the body and the viral load dropped within 1 week to levels below the limit of detection. Assuming that the detection limit represents the minimum decline after nephrectomy, a decay slope of  $-0.85$  per day could be obtained, which translated into a half-life of 20 h or less.  $R_0$  dropped to 0.2 or less after nephrectomy.

In a patient prospectively sampled with high frequency after nephrectomy (every 3 h for the first day), the viral load dropped for 6 h with an average half-life of 1.4 h. The average viral kinetics estimated from 12 patients receiving various combinations of immunosuppressive drugs were: doubling time 5 days (range 18 h to 37 days), half-life 5.5 days (range 5.5 h to 17 days).<sup>7</sup>

The general picture of BKV pathogenesis and PVAN that emerges when combining in-vivo and in-vitro data of BKV from various sources is a short viral half-life, which implies a high viral turnover of more than 99%. In-vitro experiments reported an intracellular delay of 2 days between infection of a host cell and release of infectious progeny virus.<sup>37</sup> Assuming a viral half-life of 1–2 h and a burst size of  $10^4$  progeny viruses per productively infected cell,<sup>7,84</sup> we estimate that  $10^5$  to  $10^6$  renal cells are lost every day to maintain an apparently stable viral load of around  $10^6$  copies per mL.<sup>7</sup> Because the kidney has only a finite number of host cells (tubular epithelial cells) and a presumably limited regenerative capacity, ongoing viral replication pushes the graft to a state where the target cell pool is eventually exhausted. If, for example, the overall size of the target cell pool were  $10^8$  cells, extrapolation suggests an infection duration of 3 months to 3 years. Over a period of 25 weeks with a stable viraemia of around  $10^5$  copies per mL, as shown in figure 8, 50–60 generations of lytically replicating virus follow one another with a cumulative loss of  $5 \times 10^6$  or more renal cells. The extrapolated graft survival time is 10 years or less. The examples indicate that for a cytopathic virus such as BKV, a stable viraemia in a patient is not sufficient to prevent disease progression.

Our estimate of the cytopathic contribution of BKV to PVAN is solely based on plasma virus data. By not considering viral load data from other compartments such as the urinary tract, where the viral load is usually much higher than in the plasma, it is likely that we underestimate the overall cytopathic contribution of BKV to PVAN. Hence, the projected survival time of an infected graft could well be much shorter than estimated from blood data only. Viral load dynamics of BKV in matched blood and urine samples and mathematical modelling suggest weakly linked replication compartments in vivo (Funk and Hirsch, unpublished data). Additionally, a renal allograft becomes dysfunctional well in advance before the last host cell is destroyed. As the replication kinetics of BKV become better defined, immunotherapeutic approaches should

be reconsidered to improve current post-transplant management strategies.<sup>82</sup>

### Other transplant relevant virus infections

GBV-C, previously known as hepatitis G virus, was quantified by Berg and colleagues<sup>36</sup> in 12 patients before and daily after liver transplantation for 25–28 days to test whether the liver is the principal site of replication.<sup>36</sup> Although the paper provides quantitative viral load information, decay rates were not calculated. When reanalysing the reported mean GBV-C RNA values from day –1, 1, 2, 3, 7, and 28 post-transplant, we estimated that the GBV-C half-life immediately after hepatectomy was 2.5 days or less. Between days 1 and 7, the respective half-lives were 18, 16, and 12 days. Between days 7 and 28 the viral load increased with a doubling time of 67 days. From the observed decay characteristics, the authors concluded that the liver is not the major site of GBV-C replication. This implies that the true half-life might be shorter than 2.5 days, but also that the contribution of GBV-C to liver pathology is limited. It also offers an explanation for the poor response of GBV-C to interferon- $\alpha$  therapy.<sup>85</sup>

Adenovirus has received attention because stealth adenovirus constructs are used as vectors for transgene delivery in gene therapy and oncolysis. Adenovirus type 5 is rapidly cleared from the blood of mice with a half-life of 2 min or less.<sup>86</sup> The kinetics of adenovirus in human hosts remains obscure. In paediatric transplantation, adenovirus infections cause frequent complications. The initial phase of infection may be local and asymptomatic. Simultaneous isolation of adenovirus from multiple sites (urine, stool, throat swabs) has been associated with occurrence of clinical disease, whereas isolation of adenovirus from plasma is associated with high mortality. Lankester and colleagues<sup>39</sup> quantified adenovirus loads in two paediatric stem cell transplant patients to evaluate the effect of antiviral treatment. From one patient described in the study,<sup>39</sup> we were able to estimate a viral doubling time of 1.3 days (day 48–73). The increasing adenovirus load is remarkable since treatment with cidofovir (5 mg/kg per

### Search strategy and selection criteria

Data for this Review were identified by searches of PubMed using combinations of the search terms “transplant”, “transplantation”, “kinetics”, “dynamics”, “eclipse phase”, and “intracellular delay” together with the names of the viruses described in this article. Further search terms were “EBV episomal”, “EBV circular DNA”, “EBV linear DNA”, “EBV cell free”, and “EBV cell associated”. We also included references from key articles and from our own files. If no viral kinetic data (doubling times, half-lives) were available, we selected those papers that allowed us to accurately estimate viral kinetics from viral loads reported in the text, in tables, or in figures. Only papers written in English language were considered. The final search date was March, 2006.

day) was initiated on day 59 (17 days after the second transplantation). Because the viral load further increased and clinical symptoms progressed, ribavirin was added to the antiviral treatment at day 66 (loading dose 30 mg/kg per day, maintenance dose 60 mg/kg per day), but its antiviral efficacy on adenovirus is questionable. Unfortunately, the patient died at day 78 because of fulminant adenovirus disease. In another patient, adenovirus was isolated from stool, urine, and throat swabs. However, the patient remained free of adenovirus in the plasma and clinical symptoms were restricted to a temporary form of mild diarrhoea.<sup>39</sup> From a bone marrow transplant patient described by Watzinger and colleagues,<sup>40</sup> we obtained a similar doubling time of 2.1 days (day 154–168). Our analysis shows that rapid dynamics of adenovirus can be observed in some paediatric stem cell transplant patients. Because plasma viraemia precedes onset of clinical symptoms by a median of more than 3 weeks,<sup>37</sup> frequent sampling is required to identify patients at risk of progression to fulminant disseminated disease with organ complication such as pneumonia, hepatitis, encephalitis, or fatal multi-organ failure, and to monitor pre-emptive antiviral interventions.

### Conclusion

When looking across various viral infections and different transplant settings, we see that viral replication in vivo is much more rapid than initially thought. Minimum half-lives range from less than 1 h (HCV) to 1–2 days (CMV). A direct consequence of short viral half-lives in vivo is a high daily turnover of viruses ranging from around 50% to more than 99%. Organ pathology depends partly on pathogen-related factors such as cytopathicity, the viral generation time, and turnover rate, but also on the viral load and the strength and timing of a host's immune response (the degree of immunosuppression). To identify potentially harmful infections as early as possible, blood sampling and molecular diagnostic analysis need to be optimised after transplantation and after changing immunosuppressive therapy. Efficacies of antiviral interventions can be quantified and monitored by the basic reproductive ratio  $R_0$ . For lytically replicating viruses, it might not be sufficient to achieve a stable viral load in a patient, since host cells are constantly lost and must be replenished to preserve graft function. The kinetic view suggests that disease and graft failure are correlated with the rapid replication dynamics that above a certain threshold exhaust the regenerative capacity and provoke compromising acute and chronic inflammatory responses. For viruses eliciting an only partly replication-dependent or fully replication-independent pathology, such as EBV in PTLTD, viral dynamic estimates may prove crucial to optimally interpret viral load data, risk of disease, and efficacy of treatment.

### Conflicts of interest

We declare that we have no conflicts of interest.

### Acknowledgments

We thank Alexis Dumoulin for discussing technical aspects of EBV detection and acknowledge funding from the University of Basel and the Novartis Jubilee Foundation, Basel.

### References

- 1 Oldstone MB. Viruses can cause disease in the absence of morphological evidence of cell injury: implication for uncovering new diseases in the future. *J Infect Dis* 1989; **159**: 384–89.
- 2 Hirsch HH. BK virus: opportunity makes a pathogen. *Clin Infect Dis* 2005; **41**: 354–60.
- 3 Perelson AS. Modelling viral and immune system dynamics. *Nat Rev Immunol* 2002; **2**: 28–36.
- 4 Ho DD, Neumann AU, Perelson AS, Chen W, Leonard JM, Markowitz M. Rapid turnover of plasma virions and CD4 lymphocytes in HIV-1 infection. *Nature* 1995; **373**: 123–26.
- 5 Wei X, Ghosh SK, Taylor ME, et al. Viral dynamics in human immunodeficiency virus type 1 infection. *Nature* 1995; **373**: 117–22.
- 6 Perelson AS, Neumann AU, Markowitz M, Leonard JM, Ho DD. HIV-1 dynamics in vivo: virion clearance rate, infected cell life-span, and viral generation time. *Science* 1996; **271**: 1582–86.
- 7 Nowak MA, Bonhoeffer S, Hill AM, Boehme R, Thomas HC, McDade H. Viral dynamics in hepatitis B virus infection. *Proc Natl Acad Sci USA* 1996; **93**: 4398–402.
- 8 Whalley SA, Murray JM, Brown D, et al. Kinetics of acute hepatitis B virus infection in humans. *J Exp Med* 2001; **193**: 847–54.
- 9 Neumann AU, Lam NP, Dahari H, et al. Hepatitis C viral dynamics in vivo and the antiviral efficacy of interferon-alpha therapy. *Science* 1998; **282**: 103–07.
- 10 Hirsch HH. Virus infections post transplant: risk and immunity. *Transpl Infect Dis* 2005; **7**: 97–98.
- 11 Pereyra F, Rubin RH. Prevention and treatment of cytomegalovirus infection in solid organ transplant recipients. *Curr Opin Infect Dis* 2004; **17**: 357–61.
- 12 Bonhoeffer S, Funk GA, Gunthard HF, Fischer M, Muller V. Glancing behind virus load variation in HIV-1 infection. *Trends Microbiol* 2003; **11**: 499–504.
- 13 Mellors JW, Rinaldo CR Jr, Gupta P, White RM, Todd JA, Kingsley LA. Prognosis in HIV-1 infection predicted by the quantity of virus in plasma. *Science* 1996; **272**: 1167–70.
- 14 Perelson AS, Essunger P, Cao Y, et al. Decay characteristics of HIV-1 infected compartments during combination therapy. *Nature* 1997; **387**: 188–91.
- 15 Finzi D, Siliciano RF. Taking aim at HIV replication. *Nat Med* 2000; **6**: 735–36.
- 16 Funk GA, Fischer M, Joos B, et al. Quantification of in vivo replicative capacity of HIV-1 in different compartments of infected cells. *J Acquir Immune Defic Syndr* 2001; **26**: 397–404.
- 17 Di Mascio M, Dornadula G, Zhang H, et al. In a subset of subjects on highly active antiretroviral therapy, human immunodeficiency virus type 1 RNA in plasma decays from 50 to <5 copies per milliliter, with a half-life of 6 months. *J Virol* 2003; **77**: 2271–75.
- 18 Ho DD. Toward HIV eradication or remission: the tasks ahead. *Science* 1998; **280**: 1866–67.
- 19 Rosenberg ES, Altfield M, Poon SH, et al. Immune control of HIV-1 after early treatment of acute infection. *Nature* 2000; **407**: 523–26.
- 20 Oxenius A, Price DA, Easterbrook PJ, et al. Early highly active antiretroviral therapy for acute HIV-1 infection preserves immune function of CD8+ and CD4+ T lymphocytes. *Proc Natl Acad Sci USA* 2000; **97**: 3382–87.
- 21 Markowitz M, Louie M, Hurley A, et al. A novel antiviral intervention results in more accurate assessment of human immunodeficiency virus type 1 replication dynamics and T-cell decay in vivo. *J Virol* 2003; **77**: 5037–38.
- 22 Smith LM, Tonkin JN, Lawson MA, Shellam GR. Isolates of cytomegalovirus (CMV) from the black rat *Rattus rattus* form a distinct group of rat CMV. *J Gen Virol* 2004; **85**: 1313–17.
- 23 Ghisetti V, Barbui A, Franchello A, et al. Quantitation of cytomegalovirus DNA by the polymerase chain reaction as a predictor of disease in solid organ transplantation. *J Med Virol* 2004; **73**: 223–29.
- 24 Emery VC, Hassan-Walker AF, Burroughs AK, Griffiths PD. Human cytomegalovirus (HCMV) replication dynamics in HCMV-naive and experienced immunocompromised hosts. *J Infect Dis* 2002; **185**: 1723–28.

- 25 Emery VC. Viral dynamics during active cytomegalovirus infection and pathology. *Intervirology* 1999; **42**: 405–11.
- 26 Mattes FM, Hainsworth EG, Hassan-Walker AF, et al. Kinetics of cytomegalovirus load decrease in solid-organ transplant recipients after preemptive therapy with valganciclovir. *J Infect Dis* 2005; **191**: 89–92.
- 27 Smets F, Latine D, Bazin H, et al. Ratio between Epstein-Barr viral load and anti-Epstein-Barr virus specific T-cell response as a predictive marker of posttransplant lymphoproliferative disease. *Transplantation* 2002; **73**: 1603–10.
- 28 Gärtner BC, Schafer H, Marggraf K, et al. Evaluation of use of Epstein-Barr viral load in patients after allogeneic stem cell transplantation to diagnose and monitor posttransplant lymphoproliferative disease. *J Clin Microbiol* 2002; **40**: 351–58.
- 29 Orentas RJ, Schauer DW Jr, Ellis FW, Walczak J, Casper JT, Margolis DA. Monitoring and modulation of Epstein-Barr virus loads in pediatric transplant patients. *Pediatr Transplant* 2003; **7**: 305–14.
- 30 To EW, Chan KC, Leung SF, et al. Rapid clearance of plasma Epstein-Barr virus DNA after surgical treatment of nasopharyngeal carcinoma. *Clin Cancer Res* 2003; **9**: 3254–59.
- 31 Boutolleau D, Fernandez C, Andre E, et al. Human herpesvirus (HHV)-6 and HHV-7: two closely related viruses with different infection profiles in stem cell transplantation recipients. *J Infect Dis* 2003; **187**: 179–86.
- 32 Dahari H, Major M, Zhang X, et al. Mathematical modeling of primary hepatitis C infection: noncytolytic clearance and early blockage of virion production. *Gastroenterology* 2005; **128**: 1056–66.
- 33 Ramratnam B, Bonhoeffer S, Binley J, et al. Rapid production and clearance of HIV-1 and hepatitis C virus assessed by large volume plasma apheresis. *Lancet* 1999; **354**: 1782–85.
- 34 Fukumoto T, Berg T, Ku Y, et al. Viral dynamics of hepatitis C early after orthotopic liver transplantation: evidence for rapid turnover of serum virions. *Hepatology* 1996; **24**: 1351–54.
- 35 Garcia-Retortillo M, Forns X, Feliu A, et al. Hepatitis C virus kinetics during and immediately after liver transplantation. *Hepatology* 2002; **35**: 680–87.
- 36 Berg T, Muller AR, Platz KP, et al. Dynamics of GB virus C viremia early after orthotopic liver transplantation indicates extrahepatic tissues as the predominant site of GB virus C replication. *Hepatology* 1999; **29**: 245–49.
- 37 Low J, Humes HD, Szczypka M, Imperiale M, BKV and SV40 infection of human kidney tubular epithelial cells in vitro. *Virology* 2004; **323**: 182–88.
- 38 Freimuth P. A human cell line selected for resistance to adenovirus infection has reduced levels of the virus receptor. *J Virol* 1996; **70**: 4081–85.
- 39 Lankester AC, van Tol MJ, Claas EC, Vossen JM, Kroes AC. Quantification of adenovirus DNA in plasma for management of infection in stem cell graft recipients. *Clin Infect Dis* 2002; **34**: 864–67.
- 40 Watzinger F, Suda M, Preuner S, et al. Real-time quantitative PCR assays for detection and monitoring of pathogenic human viruses in immunosuppressed pediatric patients. *J Clin Microbiol* 2004; **42**: 5189–98.
- 41 Dixit NM, Markowitz M, Ho DD, Perelson AS. Estimates of intracellular delay and average drug efficacy from viral load data of HIV-infected individuals under antiretroviral therapy. *Antivir Ther* 2004; **9**: 237–46.
- 42 Little SJ, McLean AR, Spina CA, Richman DD, Havlir DV. Viral dynamics of acute HIV-1 infection. *J Exp Med* 1999; **190**: 841–50.
- 43 Lawson CA. Cytomegalovirus after kidney transplantation: a case review. *Prog Transplant* 2005; **15**: 157–60.
- 44 Ljungman P, Griffiths P, Paya C. Definitions of cytomegalovirus infection and disease in transplant recipients. *Clin Infect Dis* 2002; **34**: 1094–97.
- 45 Reinke P, Prosch S, Kern F, Volk HD. Mechanisms of human cytomegalovirus (HCMV) (re)activation and its impact on organ transplant patients. *Transpl Infect Dis* 1999; **1**: 157–64.
- 46 Kim SJ, Varghese TK, Zhang Z, et al. Renal ischemia/reperfusion injury activates the enhancer domain of the human cytomegalovirus major immediate early promoter. *Am J Transplant* 2005; **5**: 1606–13.
- 47 Razonable RR, van Crujisen H, Brown RA, et al. Dynamics of cytomegalovirus replication during preemptive therapy with oral ganciclovir. *J Infect Dis* 2003; **187**: 1801–08.
- 48 Humar A, Kumar D, Boivin G, Caliendo AM. Cytomegalovirus (CMV) virus load kinetics to predict recurrent disease in solid-organ transplant patients with CMV disease. *J Infect Dis* 2002; **186**: 829–33.
- 49 Anderson RM, May RM. Infectious diseases of humans: dynamics and control. Oxford: Oxford University Press, 1991.
- 50 Lloyd AL. The dependence of viral parameter estimates on the assumed viral life cycle: limitations of studies of viral load data. *Proc Biol Sci* 2001; **268**: 847–54.
- 51 Boivin G, Goyette N, Gilbert C, Humar A, Covington E. Clinical impact of ganciclovir-resistant cytomegalovirus infections in solid organ transplant patients. *Transpl Infect Dis* 2005; **7**: 166–70.
- 52 Hanto DW, Gajl-Peczalska KJ, Frizzera G, et al. Epstein-Barr virus (EBV) induced polyclonal and monoclonal B-cell lymphoproliferative diseases occurring after renal transplantation. Clinical, pathologic, and virologic findings and implications for therapy. *Ann Surg* 1983; **198**: 356–69.
- 53 Walling DM, Andritsos LA, Etienne W, et al. Molecular markers of clonality and identity in Epstein-Barr virus-associated B-cell lymphoproliferative disease. *J Med Virol* 2004; **74**: 94–101.
- 54 Thorley-Lawson DA, Gross A. Persistence of the Epstein-Barr virus and the origins of associated lymphomas. *N Engl J Med* 2004; **350**: 1328–37.
- 55 Preiksaitis JK. New developments in the diagnosis and management of posttransplantation lymphoproliferative disorders in solid organ transplant recipients. *Clin Infect Dis* 2004; **39**: 1016–23.
- 56 Gustafsson A, Levitsky V, Zou JZ, et al. Epstein-Barr virus (EBV) load in bone marrow transplant recipients at risk to develop posttransplant lymphoproliferative disease: prophylactic infusion of EBV-specific cytotoxic T cells. *Blood* 2000; **95**: 807–14.
- 57 Hodgkin PD, Lee JH, Lyons AB. B cell differentiation and isotype switching is related to division cycle number. *J Exp Med* 1996; **184**: 277–81.
- 58 Wagner HJ, Fischer L, Jabs WJ, Holbe M, Pethig K, Bucsky P. Longitudinal analysis of Epstein-Barr viral load in plasma and peripheral blood mononuclear cells of transplanted patients by real-time polymerase chain reaction. *Transplantation* 2002; **74**: 656–64.
- 59 Storek J, Lalovic BB, Rupert K, Dawson MA, Shen DD, Maloney DG. Kinetics of B, CD4 T, and CD8 T cells infused into humans: estimates of intravascular:extravascular ratios and total body counts. *Clin Immunol* 2002; **102**: 249–57.
- 60 Wang J, Sugden B. Origins of bidirectional replication of Epstein-Barr virus: models for understanding mammalian origins of DNA synthesis. *J Cell Biochem* 2005; **94**: 247–56.
- 61 Laichalk LL, Hochberg D, Babcock GJ, Freeman RB, Thorley-Lawson DA. The dispersal of mucosal memory B cells: evidence from persistent EBV infection. *Immunity* 2002; **16**: 745–54.
- 62 Comoli P, Labirio M, Basso S, et al. Infusion of autologous Epstein-Barr virus (EBV)-specific cytotoxic T cells for prevention of EBV-related lymphoproliferative disorder in solid organ transplant recipients with evidence of active virus replication. *Blood* 2002; **99**: 2592–98.
- 63 Comoli P, Maccario R, Locatelli F, et al. Treatment of EBV-related post-renal transplant lymphoproliferative disease with a tailored regimen including EBV-specific T cells. *Am J Transplant* 2005; **5**: 1415–22.
- 64 Mizukawa Y, Shiohara T. Virus-induced immune dysregulation as a triggering factor for the development of drug rashes and autoimmune diseases: with emphasis on EB virus, human herpesvirus 6 and hepatitis C virus. *J Dermatol Sci* 2000; **22**: 169–80.
- 65 De Clercq E, Naesens L, De Bolle L, Schols D, Zhang Y, Neyts J. Antiviral agents active against human herpesviruses HHV-6, HHV-7 and HHV-8. *Rev Med Virol* 2001; **11**: 381–95.
- 66 Neumann AU, Lam NP, Dahari H, et al. Differences in viral dynamics between genotypes 1 and 2 of hepatitis C virus. *J Infect Dis* 2000; **182**: 28–35.
- 67 Pawlotsky JM. Hepatitis C virus genetic variability: pathogenic and clinical implications. *Clin Liver Dis* 2003; **7**: 45–66.
- 68 Kamar N, Rostaing L, Selves J, et al. Natural history of hepatitis C virus-related liver fibrosis after renal transplantation. *Am J Transplant* 2005; **5**: 1704–12.
- 69 Watashi K, Ishii N, Hijikata M, et al. Cyclophilin B is a functional regulator of hepatitis C virus RNA polymerase. *Mol Cell* 2005; **19**: 111–22.

- 70 Powers KA, Ribeiro RM, Patel K, et al. Kinetics of hepatitis C virus reinfection after liver transplantation. *Liver Transpl* 2006; **12**: 207–16.
- 71 Ballardini G, De Raffe E, Groff P, et al. Timing of reinfection and mechanisms of hepatocellular damage in transplanted hepatitis C virus-reinfected liver. *Liver Transpl* 2002; **8**: 10–20.
- 72 Karino Y, Toyota J, Sugawara M, et al. Hepatitis C virus genotypes and hepatic fibrosis regulate 24-h decline of serum hepatitis C virus RNA during interferon therapy in patients with chronic hepatitis C. *J Gastroenterol Hepatol* 2003; **18**: 404–10.
- 73 Nicleleit V, Hirsch HH, Binet IF, et al. Polyomavirus infection of renal allograft recipients: from latent infection to manifest disease. *J Am Soc Nephrol* 1999; **10**: 1080–89.
- 74 Knowles WA, Pipkin P, Andrews N, et al. Population-based study of antibody to the human polyomaviruses BKV and JCV and the simian polyomavirus SV40. *J Med Virol* 2003; **71**: 115–23.
- 75 Hirsch HH, Steiger J. Polyomavirus BK. *Lancet Infect Dis* 2003; **3**: 611–23.
- 76 Binet I, Nicleleit V, Hirsch HH, et al. Polyomavirus disease under new immunosuppressive drugs: a cause of renal graft dysfunction and graft loss. *Transplantation* 1999; **67**: 918–22.
- 77 Funk GA, Steiger J, Hirsch HH. Rapid dynamics of polyomavirus type BK in renal transplant recipients. *J Infect Dis* 2006; **193**: 80–87.
- 78 Hirsch HH, Knowles W, Dickenmann M, et al. Prospective study of polyomavirus type BK replication and nephropathy in renal-transplant recipients. *N Engl J Med* 2002; **347**: 488–96.
- 79 Randhawa PS, Finkelstein S, Scantlebury V, et al. Human polyoma virus-associated interstitial nephritis in the allograft kidney. *Transplantation* 1999; **67**: 103–09.
- 80 Hirsch HH. Polyomavirus BK nephropathy: a (re-)emerging complication in renal transplantation. *Am J Transplant* 2002; **2**: 25–30.
- 81 Hirsch HH, Drachenberg CB, Steiger J, Ramos E. Polyomavirus associated nephropathy in renal transplantation: critical issues of screening and management. *Adv Exp Med Biol* 2006; **577**: 160–73.
- 82 Hirsch HH, Brennan DC, Drachenberg CB, et al. Polyomavirus-associated nephropathy in renal transplantation: interdisciplinary analyses and recommendations. *Transplantation* 2005; **79**: 1277–86.
- 83 Drachenberg CB, Papadimitriou JC, Hirsch HH, et al. Histological patterns of polyomavirus nephropathy: correlation with graft outcome and viral load. *Am J Transplant* 2004; **4**: 2082–92.
- 84 Randhawa PS, Vats A, Zygmunt D, et al. Quantitation of viral DNA in renal allograft tissue from patients with BK virus nephropathy. *Transplantation* 2002; **74**: 485–88.
- 85 Jarvis LM, Bell H, Simmonds P, et al. The effect of treatment with alpha-interferon on hepatitis G/GBV-C viraemia. The CONSTRUCT Group. *Scand J Gastroenterol* 1998; **33**: 195–200.
- 86 Alemany R, Suzuki K, Curiel DT. Blood clearance rates of adenovirus type 5 in mice. *J Gen Virol* 2000; **81**: 2605–09.
- 87 Lion T, Baumgartinger R, Watzinger F, et al. Molecular monitoring of adenovirus in peripheral blood after allogeneic bone marrow transplantation permits early diagnosis of disseminated disease. *Blood* 2003; **102**: 1114–20.